Observed Variations of Tropical CAPE

Charlotte A. DeMott

David A. Randall

Department of Atmospheric Science
Colorado State University
Fort Collins, Colorado 80523

22 April 2003

Prepared for submission to *Journal of Geophysical Research*

Abstract

Data from selected tropical radiosonde stations (located between 25°S and 25°N) are used to compute multi-decadal trends in convective available potential energy (CAPE). Positive trends slightly outnumber negative trends, with the greatest concentration of positive trends occurring in the western Pacific Ocean and the Caribbean Sea. Analysis shows that positive and negative CAPE trends are primarily driven by same-signed trends in low-level moisture, while lapse-rate trends play a secondary role and may either increase or decrease the magnitude of the CAPE trends.

Monthly CAPE anomalies are generally positively correlated with sounding-derived precipitable water (PW) and lapse rate, as well as SSMI-derived PW for retrievals located over the sounding location. Sounding-derived PW estimates for all utilized stations, which are dominated by island and coastal locations, were averaged and compared to tropical SSMI PW estimates, which are available only over the oceans. The two time series are poorly correlated, suggesting that the limited number of sounding stations considered herein does not adequately capture tropical-wide variability.

The relationship of CAPE changes to PW and lapse rate changes is examined on a variety of timescales for evidence of quasi-equilibrium (QE) behavior, in which convection acts to maintain an approximately moist adiabatic temperature profile. Strict QE (SQE)--in which convection maintains an exactly moist adiabatic temperature profile-- is assumed in the convective parameterizations of many general circulation models (GCMs). PW and lapse rate anomalies are

negatively correlated on multi-decadal timescales and on monthly timescales in heavily raining regions, in support of QE theory. However, no such negative correlation is seen over the course of the seasonal cycle, or for monthly timescales in low-rain areas.

CAPE anomalies were compared to nearest-grid-point monthly precipitation anomalies derived from surface-based rain gauges. Correlations are small and centered about zero. Mean tropical rainfall estimates, based on a combination of satellite and surface gauge data, are uncorrelated with the mean tropical SSMI PW estimates.

1. Introduction

Because of the importance of moist convection for large-scale tropical circulations, the factors that influence the geographic and temporal variability of moist convection are key to understanding larger-scale atmospheric variability, to simulation of such variability with general circulation models (GCMs), and to interpreting and/or predicting changes in the global hydrologic cycle in the context of climate-change scenarios. Among the key factors affecting moist convection are water vapor, lapse rate, vertical motion, the surface sensible and latent heat fluxes and, perhaps most importantly, the convective available potential energy (CAPE). This paper reports on a study in which we have used observations to explore the variability of CAPE and related quantities in the tropical atmosphere, on time scales ranging from days to decades.

Daily or twice-daily radiosonde records at many tropical locations extend back as far the late 1940s. Because these observations offer in situ, high-resolution temporal and spatial sampling of the vertical temperature and moisture structures, they have recently been applied to the study of decadal variability. One result that has consistently emerged through these analyses is the presence of multi-decadal trends. For example, in his analysis of four West Pacific stations, Gutzler (1992) found positive temperature and moisture trends at all levels from 1974-1988. Further analysis (Gutzler, 1996) revealed that these trends cannot be accounted for by the accumulated effects of recent prolonged and intense El Niño-Southern Oscillation (ENSO) events, and that the 1991 eruption of Mt. Pinatubo coincided with a reduction in the trends. Gaffen et al. (2000) report that tropospheric lapse rates increased during 1979-1997, because greater warming took place at the surface than aloft. Gaffen et al. (1991) report a step-like jump in atmospheric temperature and moisture values in the late 1970's, consistent with previously

reported changes in tropical circulation patterns (e.g., Nitta and Yamada, 1989; Trenberth and Hurrell, 1994). They also report that increases in tropical moisture may be accompanied by drying in the extratropics. Similarly, Ross and Elliott (2001), examining several stations throughout the Northern Hemisphere, found that vertically integrated water vapor increased at most stations, especially over North America and the Pacific Ocean, with the greatest increases occurring since 1973.

In an effort to assess the combined effects of positive temperature and moisture trends on the regulation of convective activity, Gettelman et al. (2002, hereafter referred to as G02) computed convective available potential energy (CAPE) trends at 15 tropical sounding locations. Trends were positive at 13 of these stations, which suggests that changes in the large-scale structure of the atmosphere should be reflected in the behavior of tropical convection.

Precisely how such changes in the large-scale temperature and moisture structure of the tropical troposphere are manifested in convective activity, however, is not clear. Trenberth (1998) suggests that a warmer atmosphere may result in more water vapor remaining in the atmosphere, rather than precipitating out, so precipitation trends may not be consistent with atmospheric moisture content trends. He goes on to state that the main effect of increasing moisture content on moisture-convergence-driven rainfall production is that rain rates should increase faster than rain amounts. This statement appears to be consistent with the findings of Tsonis (1996), who finds that, although there is evidence of increasing atmospheric instability, mean global precipitation has not changed dramatically from 1890-1989. Rather, there is a distinct positive trend in the variance of precipitation.

Changes have also been observed in the tropical radiation budget. Wielicki et al. (2002) report that the longwave (LW) flux exiting the tropics has increased from 1988-1994, an increase that is not reproduced in GCMs using observed SSTs. Chen et al. (2002) suggest that these changes in LW flux are associated with a shift in the location and intensity of tropical convection, which corresponds to a strengthening of the Hadley and Walker circulations, based on increases in cloudiness and upper air relative humidity in the rising branches of these circulations, and decreases in the sinking branches. This conclusion is qualitatively consistent with the radiosonde-based results of Gaffen et al. (1991), which suggested that increases in tropical temperature and specific humidity were accompanied by decreases in these two variables in the extratropics.

In summary, the studies cited above generally indicate that 1) tropical tropospheric temperatures, moisture contents, and lapse rates have increased during the past several decades, including a step-like increase in the late 1970's, and 2) any relationships of these apparent changes in the atmospheric state to corresponding changes in the speed of the hydrologic cycle remain to be established.

Not included in the discussion up to this point, however, are the possible effects of changes in observing practices on the computed trends. While the sounding record at many stations is essentially complete for several decades, the sounding network was never designed to be used as a climate-monitoring tool. As a result, changes in observation practices (i.e., launch time, recording technique, station location, instrumentation, etc.) are frequent, and generally motivated by the desire to improve short-term forecasts, rather than to establish long-term datasets that can be used to explore climate variations. A further complication is that many different

radiosonde types are or have been used across the globe and throughout the data record (Gaffen, 1996). To add to the confusion, changes in observing practices may have a varying impact on computed trends for various locations (e.g., Elliott et al, 2002). The result of these added levels of uncertainty in the data is to make the distinction between true climate variability and instrumentation effects difficult to discern.

The observed variability discussed above is of interest in the context of numerical simulations of climate change. In one way or another, virtually all cumulus parameterizations used in GCMs tend to limit increases of the simulated CAPE. Familiar examples include the moist-convective adjustment (MCA) proposed by Manabe et al. (1965), which assigns moist-adiabatic lapse rates to convectively adjusted layers, and the Arakawa-Schubert parameterization, which in its original form sets the cloud work function to small prescribed constant values for all active cloud types in a convectively adjusted column (Arakawa and Schubert, 1974; Lord and Arakawa, 1980). When they are used in GCMs, both MCA and the Arakawa-Schubert parameterization force the simulated sounding in regions of deep tropical convection to *approximate* (virtual) saturated moist adiabats that pass through the surface temperature and pressure (e.g., Xu and Emanuel, 1989).

The assumption that the large-scale sounding *exactly* follows a saturated moist adiabat that passes through the surface temperature and pressure is called "strict quasi-equilibrium" (SQE) by Brown and Bretherton (1997). Based on an analysis of observations, Brown and Bretherton

(1997) reported that SQE is approximately satisfied only in heavily raining areas, and that the assumption of SQE predicts too much warming aloft for a given observed increase in boundary-layer equivalent potential temperature.

Because the moist adiabatic lapse rate decreases with increasing temperature, GCMs predict that warming at the surface in the tropics will be accompanied by stronger warming aloft (e.g. Soden, 2000). Large-scale dynamics ensures that very similar temperature profiles are found throughout the tropics above the trade inversion (Charney, 1963), so that the simulated enhanced warming aloft is pervasive. Such an upper-level warming favors more infrared emission to space, thus providing a negative "lapse-rate feedback" that tends to resist further warming.

The degree to which the middle troposphere has warmed over the past two decades has been the subject of intense debate in recent years, as detailed in a report by the National Research Council (NRC, 2000) and the references contained therein. Estimates of mid-tropospheric warming during the satellite record (1979-present) suggest that the mid-troposphere has warmed at a slower rate (0.0 to 0.2 K decade^{-1}) than the surface (0.25 to 0.4 K decade^{-1}). These findings are in conflict with the model results mentioned above, suggesting that the negative lapse-rate feedback produced by the models may be exaggerated. The convection parameterizations of the GCMs are one obvious possible cause of the apparent discrepancies between the model results and observations.

The goals of this paper are 1) to study the multidecadal behavior of tropical CAPE computed from the radiosonde data set, and 2) to explore the relationship of CAPE to precipitable water, temperature lapse rate, and precipitation on a variety of time scales. The paper is organized

as follows: Section 2 discusses data selection, analysis methods, and quality-control issues. Section 3 presents our results for CAPE trends. Section 4 examines the observed relationships among CAPE, precipitable water, and lapse rate on monthly to decadal time scales. Section 5 explores the relationship between CAPE changes and precipitation. Section 6 gives a summary and conclusions.

2. Data Processing

Sounding stations within 25^{o} of the Equator were drawn from Global Climate Observing System (GCOS) Upper Air Network (GUAN) subset of the Comprehensive Aerological Research Data Set (CARDS, Eskridge et al. 1995). The GUAN stations were selected for their completeness and length of record, as well as their geographic distribution. Through the CARDS project, data from all stations were subjected to the quality control procedures described in Eskridge et al. (1995) which include correcting errors in geopotential height, temperature, humidity and wind. It should be noted, however, that biases associated with changes in observation practice or location are usually well within the observed limits of natural variability of these variables so the quality control procedures do not address these types of errors. Finally, we note that the CARDS dataset used in this analysis was found to have some problems, and is being re-quality controlled (Durre, 2002; personal communication) and available sometime in the future. It is not clear what, if any, impact the new dataset will have on these results.

For each station, every sounding was screened for appropriateness for the CAPE computation. Data at individual reporting levels were thrown out if the temperature or pressure data quality was listed as missing or suspect. The remaining levels were then examined as a whole

and the entire sounding was thrown out if any of the following conditions were met: 1) the first data level was more than 50 m above the surface, 2) the sounding terminated before reaching 200 mb, 3) more than 20% of mandatory reporting levels below 200 mb were missing, 4) missing or suspect relative humidity data was reported at the first two retained data levels, or 5) the balloon descended prior to reaching the tropopause or 200 mb, whichever came last.

Soundings were then divided into two groups based on launch time (00 Z +/- 2 hours and 12 Z +/- 2 hours). For each launch time, time series were plotted for the number of observations per month, the annual mean near-surface temperature and relative humidity (defined by the level closest to 15 mb above the surface). The times of known observation practice changes were indicated (Gaffen, 1996). Time series were then subjectively evaluated based on the following criteria:

1. The time series must extend back at least 20 years from December 1999.

2. The number of observations per month must be reasonably uniform and should meet or exceed 10 samples per month. (A typical sampling density is 20~30 samples per month.)

3. Gaps (missing data) should not exceed 18 months duration individually or 4 years (for a 20 year record) collectively.

4. Following the practice of G02, time series were eliminated or truncated if the annual mean deviations in the near-surface temperature or humidity exceeded 1-σ of the long-term

mean for more than four years beyond a documented change in station location, instrumentation, or observing practice.

Locations of the stations whose time series met all of these criteria are shown in Fig. 1 and the exact date ranges used in the trend calculation are summarized in Table 1. Although data coverage in many parts of the tropics is minimal, the locations of the stations used in this analysis are fairly representative of the number of CARDS stations available by geographic region. Note that stations are most densely clustered in the Maritime Continent-West Pacific regions and the Caribbean Sea.

At this point, it is appropriate to include some discussion of the impacts of observation practice changes on temperature and moisture measurements which, in turn, affect the CAPE computation. CAPE is the vertical integral of parcel buoyancy, which is a function of parcel moisture content, and atmospheric temperature profile. Radiosondes provide vertical profiles of temperature and moisture, which are subject to instrumentation errors. Efforts to ascertain errors associated with instrumentation and/or launch location changes have focused primarily on the impact such changes have on temperature and moisture measurements. In their study of the sensitivity of tropospheric temperature trends to radiosonde data quality, Gaffen et al. (2000) list completeness of the data time series, choice of radiosonde dataset used in trend computation, and the statistical method used to compute the trend as having a small impact on the computed trend. The major impact on computed trends was from instrumentation changes. By employing the non-parametric statistical techniques of Lanzante (1996) combined with historical station metadata to adjust the data for instrumentation-related discontinuities, the authors found that the temperature

trends were generally still present, but reduced. While this is encouraging, the fact remains that undocumented instrumentation and/or location changes may exist in the metadata. Free et al. (2002) summarized the efforts of several groups working to identify and correct these changes and reported that, while various methods to detect undocumented change points work better than others, no one method works best. Furthermore, various methods may identify different change points as well as suggest different-signed corrections to the same change point. Recently, Lanzante et al. (2003) have estimated the impacts of observation method changes on temperature trends across the globe by adjusting temperature time series at identified change points. They find that, on average, the magnitude of needed adjustment increases from the lower to the upper troposphere and results in increased tropospheric warming of ~10%, although the results are not uniform geographically.

Instrumentation changes may also have a significant impact on moisture measurements. In their thorough analysis of tropospheric water vapor trends, Ross and Elliott (2001) present several arguments suggesting that, overall, changes in instrumentation have actually resulted in an underestimate of tropospheric moisture trends. In a general sense, changes in sonde-based humidity sensors have been driven by a desire to improve these sensors' response times. Sensors with slow response times result in high moisture biases with increasing height, given the typical decrease of water vapor with height. As humidity sensors have improved, this high bias has diminished with time, yet positive moisture trends are still observed. The authors also make extensive use of the aforementioned non-parametric tests to test for outliers and change points in the time series. They use results of these tests to estimate the fraction of trend that might be accounted for by undetected instrument changes and find that such instrument-related

contributions alone cannot account for the increase in Northern Hemisphere water vapor, which is especially significant over North America and the Pacific Ocean. Considering these results in conjunction with the enhanced tropical tropospheric warming reported in Lanzante et al. (2003), as well as the evidence supporting the idea of a constant relative humidity atmosphere (e.g., Wentz and Schabel, 2000) this appears to be a reasonable conclusion.

The preceding discussion shows that careful selection of sounding stations and time series truncation are essential in order to obtain reliable CAPE trends. Given such quality control measures, the computed trends should be at least qualitatively accurate. With these caveats in mind, we computed trends in tropical CAPE and analyzed them quantitatively, but we acknowledge that our results should only be interpreted in a qualitative manner.

We compute CAPE values for every sounding that was retained in the sounding screening process. Data were first interpolated to 10 mb resolution, a practice that reduces the tendency for CAPE to decrease with increasing vertical sampling resolution (Gettelman et al., 2002). For our purposes, we report only the "positive" CAPE values for a parcel lifted from the level closest to 15 mb above the surface. Probability distribution functions (PDFs) of CAPE for all twelve calendar months were constructed based on the entire time series. Values exceeding +/- 2 standard deviations were eliminated. Monthly CAPE anomalies were computed relative to the average values over the time series for the same-named month. Trends were then computed by regressing the monthly anomalies in time, using a least-squared fit. The trends were evaluated for statistical significance using a two-tailed Student's t-test at the 95% confidence level.

3. CAPE trends

Fig. 1 shows the CAPE trends for 00Z and 12Z launch times, based on the entire length of record retained for the analysis (1973-1999). We have focused on the post-1973 time period, as have other users of this dataset (e.g., Gaffen et al., 1991), because this date marks the last major change to recording practices of United States-provided radiosonde instruments. Although several non-US stations are included in the analysis, we focus on the 1973-1999 time period so that trends among stations are as directly comparable as possible. The exact date ranges of each station analyzed are summarized in Table 1. The magnitudes of the trends are expressed as percentages of the raw time series mean values per decade. This facilitates comparison with earlier studies, although it may mask large absolute changes in CAPE, and may comparatively inflate small absolute changes. Of the 31 stations analyzed, 18 have positive CAPE trends and 13 have negative CAPE trends. For the 9 stations that launch soundings twice per day, all have same-signed trends for 00Z and 12Z launch times. When considering only those stations with statistically significant CAPE trends, positive trends outnumber negative trends by about 3:2.

Geographically, positive trends tend to be clustered in the West Pacific-Maritime Continent region north of the Equator, and in the Caribbean. Clusters of negative trends are found in and around the African continent, the northern half of Australia, and the western subtropical Pacific Ocean. The case for negative clusters is less convincing than that for positive clusters, however, as the station density is less in these regions, and there is a mixture of positive and negative trend stations in these areas. Certainly, there appears to be no zonally uniform increase or decrease in CAPE based on the stations analyzed.

In an overall sense, CAPE trend results compare well with those presented in G02, despite the fact that the two studies used slightly different sets of stations. Ten stations are common to the two studies, and same-signed trends are reported at nine of the stations. In G02's Fig. 3, CAPE trends are positive at 12 of the 15 stations analyzed, and from this they concluded that "there have been significant changes to the convective stability of the tropical atmosphere...over the 40 year period examined." In our Fig. 1, however, 58% of all stations exhibited positive CAPE trends, and 42% exhibited negative trends. Our results do not provide evidence for any systematic global CAPE trends. Reasons for this discrepancy are discussed in Section 6.

4. CAPE vs. precipitable water, lapse rate

Because CAPE is a function of lifted parcel moisture content and atmospheric lapse rate, we next examine the relationships between these two variables and CAPE. Water vapor content is represented in terms of precipitable water (PW) content, which we computed by vertically integrating the sounding-derived water vapor mixing ratio profile. Because water vapor mixing ratios are highest at low levels, PW is most sensitive to near-surface water vapor contents, which is also the level from which the parcel is lifted in the CAPE calculation. Low-level (surface to 700 mb) and mid-level (700-300 mb) lapse rates (dT/dz) have also been computed from the sounding data. Monthly anomalies are determined as with the CAPE data.

Are CAPE trends driven primarily by lapse rate changes, or by increased low-level water vapor contents? To address this question, we partitioned the trend in CAPE into the parts that are explained by the trend in PW and surface-to-700 mb lapse rate, respectively. This was done by regressing the monthly anomaly CAPE time series onto the monthly PW or lapse-rate anomaly

time series, and computing a new CAPE anomaly time series based on just PW or lapse rate. The fraction of CAPE trend explained (expressed as a percentage of actual CAPE trend) is computed by dividing either the PW-predicted or lapse rate-predicted CAPE trend by the actual CAPE trend. A negative fraction results when the sign of the actual trend is opposite the sign of the predicted trend. Fig. 2 compares the fraction of CAPE trend accounted for by PW trends with the fraction accounted for by low-level lapse-rate trends. Results for mid-level lapse rates (not shown) are similar, but the percentages are generally lower. Stations with positive (negative) trends in CAPE are indicated with circles (diamonds). Filled (open) symbols indicate statistically significant (not significant) CAPE trends.

Except for one station, positive CAPE trends are associated with positive PW trends. Moreover, the PW trend is the dominant factor in determining the sign of the CAPE trend, as can be seen by the fact that the majority of data points are found between the 1:1 and 1:-1 lines. For about half of these stations, the portion of the CAPE trend explained by the lapse-rate trend is negative, so that CAPE increases caused by increasing surface moisture are partially offset by decreasing atmospheric instability. For the remaining stations with positive CAPE trends, lapse-rate trends either reinforce or dominate the positive CAPE trends. Stations with negative CAPE trends, however, are somewhat more likely to respond primarily to lapse-rate trends than to PW trends. Four stations exhibit CAPE trends of opposite sign than what would be suggested by both PW and lapse rate changes (points that lie in the lower left quadrant of the figure). One of two explanations exist for this inconsistency. For the one statistically significant point, the CAPE trend

arises from the 700~300 mb lapse rate trend, which is not plotted here. The remaining three stations in this quadrant exhibit statistically insignificant trends in CAPE, PW, and lapse rate, so the plotted relationship among these trends is statistically not meaningful.

The fact that over half of the sounding stations analyzed in this study exhibited statistically significant increases in CAPE led us to wonder to what extent SQE is manifested on various timescales and under various precipitation conditions. We have analyzed changes in CAPE as functions of PW and lapse rate changes for a variety of timescales and for low- and moderate-rainrate conditions. The results of this analysis are summarized in Fig. 3. Fig. 3a shows the relationship between trends in monthly anomalies of PW, lapse rate and CAPE from 1973-1999. Positive CAPE trends are most often accompanied by positive PW and negative lapse rate trends, broadly consistent with SQE, although there is a large amount of spread in the data points. On the other hand, the annual cycles of PW, lapse rate, and CAPE for each season (Fig. 3b) clearly show a positive relationship between PW and lapse rate, suggesting that the factors that determine the mean monthly values of each of these quantities can act in opposition to SQE. Even considering only the high rain months (solid circles) in Fig. 3b, there is no average tendency for a negative PW-lapse rate relation on a station by station basis. Both positive and negative relations are found across the spectrum of PW contents, but the number of months exhibiting a positive relation outnumbers the number of months exhibiting a negative relation.

A similar analysis for monthly anomalies of each variable is presented in Figs. 3c and 3d. The data are partitioned by mean monthly rainfall amount using Global Precipitation Climatology Project (GPCP) data (Adler et al., 2003) using the thresholds indicated (expressed in units of mm

day^{-1}). Monthly PW and lapse rate z-scores for any occurrence that satisfies the rainfall criteria are plotted in the appropriate panel. In moderate- to heavily-raining regions (Fig. 3c) PW and lapse rate anomalies are weakly, but significantly negatively correlated (r=-0.19 and r=-0.24 for positive and negative CAPE anomalies, respectively, using a 1-tailed Student's t-test at 95% confidence interval), as would be predicted by SQE. The large amount of scatter in the data points probably arises from the monthly averaging that was employed in generating this figure. While average monthly rainrates may exceed 3 mm day^{-1}, only a few rainy days per month may be responsible for the monthly mean being partitioned in this manner. Daily partitioning may result in higher correlations. In low rainrate regions (Fig. 3d), we essentially find no relationship, as the correlations for both positive and negative CAPE trends are not significant.

From these results, it appears that the annual cycle exhibits the strongest influence on the variability of PW and lapse rate, and that this variability bears no resemblance to that predicted by SQE. On the other hand, departures from the annual mean PW-lapse rate relationship (monthly anomalies and long-term trends; Figs. 3c and 3a) appear to be consistent with SQE in moderately- to heavily-raining regions. Low-rain regions (Fig. 3d), however, do not exhibit this behavior. These results support the findings of Brown and Bretherton (1997), namely that SQE is approximately satisfied in heavy-rain areas, but not in low-rain areas. The covariability of CAPE and precipitation is explored in the next section.

5. Relation of CAPE to precipitation

How CAPE trends should relate to precipitation trends is not clear. On one hand, CAPE is a prerequisite for convection, so increases in CAPE might be expected to be associated with greater precipitation totals. On the other hand, convective activity destroys CAPE, so long-term increases in CAPE could be associated with decreases in precipitation. Increases of the precipitation rate coupled with decreases in CAPE would be consistent with the observations of Thompson et al. (1979) and Brown and Bretherton (1997).

In many numerical models, QE closure of Arakawa and Schubert (1974) is used, as an approximation, to determine the convective heating and drying rates over a particular time step (say, one hour) and averaged over a particular grid cell (which might have an area on the order of 10^4 km^2). In QE, the actual time rate of change of the CAPE (or of a closely related quantity such as the cloud work function) is neglected in comparison to the convective tendency of the CAPE. This is only an approximation; no claim is made that the time rate of change of the CAPE is exactly zero. Over a sufficiently long time (days or months or years), the CAPE can change by an arbitrarily large amount even if the approximation used in the numerical model is quite accurate. For example, suppose that at a particular time and place the CAPE is 1000 J kg^{-1}, the actual time rate of change of the CAPE is 1 J kg^{-1} hour^{-1}, while the convective tendency of the CAPE is 100 J kg^{-1} hour^{-1}. Then the QE closure introduces an error on the order of 1%, which may be considered quite acceptable. Nevertheless, a tendency of 1 J kg^{-1} hour^{-1} for a month would give an

accumulated change of 720 J kg^{-1} -- an order 1 change in the CAPE. The point is that the QE closure can be a useful approximation (i.e., it can be "valid") even though the CAPE changes on longer time scales.

We have examined the relationship of CAPE trends to precipitation trends on local scales, as well as averaged over the entire tropics. We use gridded raingauge precipitation data from the Global Historical Climatology Network (GHCN, Vose et al., 1992; Peterson and Easterling, 1994). GHCN data are from surface-based raingauges across the globe. The data were obtained from the National Climatic Data Center (NCDC) on a 5^{o}x5^{o} grid as percent deviations from the 1961-1999 mean (Lawrimore, 2002, personal communication), thus enabling the calculation of trends with the normalized units of percent change per decade.

1973-1999 CAPE trends are plotted with GHCN precipitation trends (in units of % deviation) in Fig. 4. Only those grid points that average at least six months of observations per year are used to compute the precipitation trends. Although the primary focus of this study is on the tropics, we note that the global pattern of precipitation trends closely resembles global rainfall anomaly patterns associated with the El Niño-Southern Oscillation (ENSO) phenomenon. Specifically, the increased precipitation in the South Pacific Convergence Zone (SPCZ), straddled by two lobes of precipitation decrease in the northern and southern tropical Pacific, has been recognized as a characteristic signature of ENSO-induced precipitation variability (Morrissey and Graham, 1996; Folland et al, 2002).

A visual comparison suggests a weak tendency for CAPE and precipitation trends to be negatively correlated in the Pacific Ocean, and positively correlated in the Caribbean, with most other locations showing no clear relationship between the two. To better assess the relationship, we plot CAPE trends against the precipitation trend at the station that is the nearest neighbor to the sounding station within a 10^{o} radius (Fig. 5). The lack of relationship between the two variables is apparent; they are correlated only at $r = 0.15$, which is well below the two-tailed 95% confidence level of $r = 0.48$. Even on a region-by-region basis, there is no strong relationship between precipitation trends and CAPE trends. In fact, the main conclusion to be drawn from this figure is that CAPE trends during the 1973-1999 period are generally much stronger than precipitation trends during the same period, as evidenced by the majority of data points lying between the 1:1 and 1:-1 lines in Fig. 5. Because the GHCN precipitation dataset may be subject to artificial trends as various gages enter or exit the data assimilation, we repeated this analysis using SSMI precipitation estimates from Wilheit et al. (1991) and Wentz et al. (1998). Although there is some variability in precipitation trends among the data sets for points located over sounding stations, we still find that CAPE trend magnitudes exceed precipitation trend magnitudes for the majority of stations. This finding is generally consistent with the suggestion by Trenberth (1998) that tropospheric moisture tends to increase faster than rainfall. We caution, however, that our results are based on a very small sample.

Given the ENSO-like pattern of rainfall trends, it is probable that additional positive precipitation trends are occurring farther east than the Pacific raingauge network samples. To extract the maximum possible information from the gauge-based data, we follow the approach of Soden (2000), in which point data are averaged throughout the tropics to reduce errors associated

with moisture transport. While this practice does not eliminate the effects of moisture transport into and out of the tropics, Soden (2000) found that his conclusions were insensitive to latitudinal boundary designation. Tropical mean CAPE and GHCN precipitation are also compared to rainfall trends based on Global Precipitation Climatology Project (GPCP) Version 2 satellite estimates (Susskind et al, 1997). This data has the advantage of global coverage, but the time series is relatively short.

Before examining tropical mean variability, we present results of basic comparisons between various sounding-derived quantities and satellite-estimated quantities for grid points centered over specific sounding locations. The purpose of this exercise is simply to gain a sense of how comparable such different measurements techniques may be. The Special Sensor Microwave Imager (SSMI) instruments aboard Defense Meteorological Satellite Program (DMSP) platforms provide 2.5^{o} x 2.5^{o} oceanic precipitable water estimates from July 1987 to the present, except during a period of instrument failure from July 1990 through December 1991 (Alishouse et al, 1990). The algorithm used to compute PW from SSMI data is based on a short period (June 1987 - April 1988) of intercomparison with sounding-derived PW estimates from twenty stations, so the total SSMI PW time series is nearly independent of concurrent sounding-derived PW estimates. The GPCP dataset provides 1^{o} x 1^{o} global rainfall estimates. Oceanic rainfall estimates after 1987 are based primarily on SSMI measurements, while land-based precipitation estimates are primarily based on gauge measurements.

Fig. 6 presents histograms of correlations between monthly anomalies of sounding-derived CAPE, PW, and lapse rate and GPCP precipitation and PW for grid points centered over sounding stations from January 1988 to December 1999. Sounding- and SSMI-derived PW estimates (Fig 6a) are generally positively correlated, with 70% of stations exceeding $r = 0.6$. As expected, sounding-derived CAPE is well-correlated with sounding-derived lapse rate and precipitable water (Figs. 6b and 6c). A comparison between CAPE and SSMI-derived PW (Fig. 6d) shows that over 75% of grid points are positively correlated (only coastal and island stations are used for this comparison). Based on these first four panels, it appears that CAPE and PW estimates derived from the sounding data are in general agreement with those inferred from (for CAPE) or based on (for PW) satellite PW data. Because tropical GPCP estimates during this period are largely based on SSMI data, we expect SSMI PW and GPCP to be highly correlated (Fig. 6e).

When comparing CAPE and GPCP rainfall (Fig. 6f), however, we are again confronted with a weak correlation between these two variables, despite the relatively high correlation between CAPE and SSMI PW (Fig. 6d) and SSMI PW and GPCP rainfall (Fig. 6e). It is not entirely clear why these correlations should be so much lower than those in the other panels, but it cannot be explained by the inclusion of inland stations in Fig. 6f and their exclusion in Fig. 6e, for repeating the analysis of Fig. 6f using only inland stations or only island stations produces a similar distribution (not shown). It is also unlikely that the non-normal distribution of rainfall is the reason for the low correlation, as we have correlated monthly rainfall anomalies (about the monthly mean), which are nearly normally distributed with only a slight skew toward positive anomalies.

In an effort to reduce possible influences of moisture transport on our point analysis of CAPE and precipitation, we next turn our attention to time series of tropical-mean variables. Our approach is to compute the mean CAPE anomaly and sounding-derived PW time series based on all stations and times and to compare these to time series of GPCP precipitation and SSMI PW averaged over all tropical longitudes from 25°N to 25°S. This exercise serves two purposes; first, since sounding-derived PW is well-correlated with SSMI PW at individual grid points, the correlation between the two tropical mean time series will provide some indication of how representative our individual stations are to the overall tropics. Second, because CAPE and PW (both from soundings and SSMI) are generally positively correlated for the grid points studied, the correlation between tropical mean SSMI PW and GPCP rainfall may provide some insight into the relationship between CAPE and precipitation rate. A word of caution is warranted when making comparisons to the SSMI PW estimates, as data from different satellites are used throughout the record of this dataset, so there may be effects from instrumentation changes on the time series. However, given the high correlation between sounding-derived and SSMI PW estimates, we feel that any such instrument-related effects are minimal for this particular exercise.

Tropical mean time series of each of the above variables are presented in Fig. 7. For this figure, tropical latitudes are defined as those equatorward of 25°, but the results are qualitatively similar for other boundary choices between 15° and 40°. A comparison of mean sounding-derived PW for coastal and island stations only (Fig. 7b) and mean oceanic SSMI PW (Fig. 7a) reveals that the two series do not bear much resemblance to each other, even at the lowest frequencies. Indeed, their correlation is only $r = 0.12$. Assuming $N = 20$ based on the SSMI PW

decorrelation timescale of 5 months, this correlation coefficient is not significant at the 95% confidence level. Similarly, CAPE (Fig. 7d) and SSMI PW also bear little resemblance to each other ($r = -0.11$). Although we have not included land areas in this analysis, by limiting the sounding stations to only coastal and island locations, we argue that a mean sounding-based PW time series based on a sufficiently dense network of stations would closely resemble the mean SSMI-based time series, as suggested by Fig. 6a. However, as Fig. 7 demonstrates, this is not the case. Therefore, we should not assume that any conclusions, such as long-term trends, based solely on the sounding stations considered in this study apply to the tropics as a whole.

Because SSMI PW estimates are available only over the oceans, GPCP rainfall estimates are divided into land and ocean components (Figs. 7c and 7e). Mean oceanic and terrestrial rainfall rates are uncorrelated ($r = -0.19$) and have statistically significant opposite-signed trends (although the land-ocean combined time series has no significant trend). Mean SSMI PW is essentially uncorrelated wit both mean oceanic rainfall ($r = -0.09$) and mean terrestrial rainfall ($r = 0.13$), suggesting once again that the relationship between precipitation and CAPE is weak.

6. Summary and conclusions

CAPE trends have been computed for 31 tropical sounding locations between 25°N and 25°S for the period 1973-1999. Stations were selected based on the length and completeness of their time series record and absence of biases introduced by data recording practice changes. Positive trends slightly outnumber negative trends, but sounding- and satellite-based PW estimate comparisons suggest that the number of stations used in this study is not sufficient to be considered representative of the tropics as a whole. Average (median) positive and negative trends

are 13.4% (11.5%) decade^{-1} and -15.9% (-10.5%) decade^{-1}, respectively. Statistically significant trends were observed at 11 of 31 stations for positive trends, and 7 of 31 stations for negative trends.

Both positive and negative CAPE trends are primarily associated with trends in precipitable water, which is primarily influenced by low-level moisture. This result is consistent with the findings of Williams and Renno (1993) and Ye et al. (1998). In percentage terms, trends in atmospheric lapse rates play a secondary role in determining CAPE trends, and either enhance or reduce CAPE trends at particular stations, in approximately equal numbers.

The relationship of the variability of CAPE to PW and lapse rate changes, and its consistency with the quasi-equilibrium assumption, has been explored for a variety of timescales. Over the course of the annual cycle at all stations examined, PW and lapse rate are positively correlated, suggesting that SQE cannot account for the observed seasonal changes. However, multi-decadal trends in CAPE behave in a manner broadly consistent with SQE; in particular, positive PW trends are accompanied by negative lapse rate trends, and vice versa. Similar behavior is seen for monthly anomalies of CAPE, PW, and lapse rate in heavily raining regions, but not in regions with light or little rainfall.

CAPE time series were compared to SSM/I PW and GPCP precipitation time series to investigate how CAPE trends are related to trends in the hydrological cycle. On a station-by-station basis, CAPE is generally highly correlated with PW. However, CAPE and precipitation are essentially uncorrelated or slightly negatively correlated, both on a grid-point-by-grid-point basis and, when using SSM/I PW as a proxy for CAPE, for the tropics as a whole.

The above findings raise several questions. First, how closely does the QE behavior in both heavily and lightly raining regions approximate SQE, the condition imposed in some GCM simulations? Does the SQE assumption cause GCMs to artificially underestimate the observed trends in CAPE? What can explain the low correlation between CAPE and rainfall? These questions will be the focus of a future study.

Acknowledgements

We thank David Thompson, Dian Seidel, and Paul Ciesielski for their helpful comments and assistance. This research was supported by NASA Grant NAG5-11737.6. SSM/I data and images are produced by Remote Sensing Systems and sponsored by the NASA Pathfinder Program for early Earth Observing System (EOS) products. The authors wish to thank the Distributed Active Archive Center (Code 902) at the Goddard Space Flight Center, Greenbelt, MD, 20771, for distributing the GPCP SSM/I data; and the science investigator, Dr. Alfred Chang of the Hydrological Sciences Branch, Code 974, NASA Goddard Space Flight Center, Greenbelt, MD 20771, for producing these data products. Goddard's contribution to these activities was sponsored by NASA's Mission to Planet Earth program. Jay Lawrimore of NOAA's NCDC graciously provided assistance with the GHCN precipitation dataset. Imke Durre, also of NOAA NCDC, patiently answered many questions about the CARDs dataset. This manuscript was thoughtfully reviewed by three anonymous reviewers whose questions and suggestions resulted in several improvements.

References

Adler, R.F., G.J. Huffman, A. Chang, R. Ferraro, P. Xie, J. Janowiak, B. Rudolf6, U. Schneider, S. Curtis, D. Bolvin, A. Gruber, J. Susskind, and P. Arkin, 2003: The Version 2 Global Precipitation Climatology Project (GPCP) Monthly Precipitation Analysis (1979-Present). *J. Hydrometeor.*, to appear.

Alishouse, J.C., S. Snyder, J. Vongsathorn, and R.R. Ferraro, 1990: Determination of oceanic total precipitable water from the SSM/I. *IEEE Trans. Geo. Rem. Sens.*, **28**, 811-816.

Arakawa, A., and W. H. Schubert, 1974: The interaction of a cumulus cloud ensemble with the large-scale environment, Part I. *J. Atmos. Sci.*, **31**, 674-701.

Brown, R. G. and C. S. Bretherton, 1997: A test of the strict quasi-equilibrium theory on long time and space scales. *J. Atmos. Sci.* **54**, 624-638.

Charney, J. G., 1963: A note on large-scale motions in the tropics. *J. Atmos. Sci.*, **20**, 607-609.

Chen, J., B. E. Carlson, and A. D. Del Genio, 2002: Evidence for strengthening of the tropical general circulation in the 1990s. *Science*, **295**, 838-841.

Elliott, W. P., R. J. Ross, and W. H. Blackmore, 2002: Recent changes in NWS upper-air observations with emphasis on changes from VIZ to Vaisala radiosondes. *Bull. Amer. Meteor. Soc.*, **83**, 1003-1017.

Eskridge, R. E., O. A. Alduchov, I. V. Chernykh, Z. Panmao, A. C. Polansky, and S. R. Doty, 1995: A comprehensive aerological reference data set (CARDS): Rough and systematic errors. *Bull. Amer. Meteor. Soc.*, **76**, 17569-1775.

Folland C.K., J. A. Renwick, M. J. Salinger, and A. B. Mullan, 2002: Relative influences of the Interdecadal Pacific Oscillation and ENSO on the South Pacific Convergence Zone. *Geophys. Res. Lett.*, **29**, 21-1 - 21-4.

Free, M., I. Durre, E. Aguilar, D. Seidel, T. C. Peterson, R. E. Eskridge, J. K. Luers, D. Parker, M. Gordon, J. Lanzante, S. Klein, J. Christy, S. Schroeder, B. Soden, L. M. McMillin, and E. Weatherhead, 2002: Creating climate reference datasets: CARDS workshop on adjusting radiosonde temperature data for climate monitoring. *Bull. Amer. Meteor. Soc.*, **83**, 891-899.

Gaffen, D. J., T. P. Barnett, and W. P. Elliott, 1991: Space and time scales of global tropospheric moisture. *J. Climate.*, **4**, 989-1008.

Gaffen, D. J., 1996: A digitized metadata set of global upper-air station histories. NOAA Tech. Memo. ERL ARL-211, 38 pp.

Gaffen, D. J., B. D. Santer, J. S. Boyle, J. R. Christy, N. E. Graham, and R. J. Ross, 2000: Multidecadal changes in the vertical temperature structure of the tropical troposphere. *Science*, **287**, 1242-1245.

Gaffen, D. J., M. A. Sargent, R. E. Habermann, and J. R. Lanzante, 2000: Sensitivity of tropospheric and stratospheric temperature trends to radiosonde data quality. *J. Climate*, **13**, 1776-1796.

Gettelman, A., D. J. Seidel, M. C. Wheeler, and R. J. Ross, 2002: Multi-decadal trends in tropical convective available potential energy. *J. Geophys. Res.*, in press

Gutzler, D. S., 1992: Climatic variability of temperature and humidity over the tropical western Pacific. *Geophys. Res. Lett.*, **19**, 1595-1598.

Gutzler, D. S., 1996: Low-frequency ocean-atmosphere variability across the tropical western Pacific. *J. Atmos. Sci.*, **53**, 2773-2785.

Lanzante, J. R., 1996: Resistant, robust and non-parametric techniques for the analysis of climate data: Theory and examples, including applications to historical radiosonde station data. *Int. J. of Climatol.*, **16**, 1197-1226.

Lanzante, J. R., S. A. Klein, and D. J. Seidel, 2003: Temporal homogenization of monthly radiosonde temperature data. Part II: Trends, sensitivities, and MSU comparison. *J. Climate*, **16**, 241-262.

Lord, S. J., and A. Arakawa, 1980: Interaction of a cumulus ensemble with the large-scale environment. Part II. *J. Atmos Sci.*, ***37*,** 2677-2692.

Manabe, S., J. Smagorinsky, and R. F. Strickler, 1965: Simulated climatology of a general circulation model with a hydrologic cycle. *Mon. Wea. Rev.*, **93**, 769-798.

Morrissey, M. L., and N. E. Graham, 1996: Recent trends in rain gauge precipitation measurements from the tropical Pacific: Evidence for an enhanced hydrologic cycle. *Bull. Amer. Meteor. Soc.*, **77**, 1207-1219.

National Research Council, 2000: Reconciling observations of global temperature change. National Academy Press, Washington D.C., 85 pp.

Nitta, T., and S. Yamada, 1989: Recent warming of tropical sea surface temperature and its relationship to the Northern Hemisphere circulation. *J. Meteorol. Soc. Japan*, **67**, 375-383.

Peterson, T. C. and D. R. Easterling, 1994: Creation of homogeneous composite climatological reference series. *International J. Climatology*, **14**, 671-679.

Ross, R. J. and William P. Elliott, 2001: Radiosonde-based northern hemisphere tropospheric water vapor trends. *J. Climate*, **14**, 1602-1612.

Soden, B. J., 2000: The sensitivity of the tropical hydrological cycle to ENSO. *J. Climate*, **13**, 538-549.

Susskind, J., P. Piraino, L. Rokke, L. Iredell, and A. Mehta, 1997: Characteristics of the TOVS Pathfinder Path A dataset. *Bull. Amer. Meteor. Soc.*, **78**, 1449-147.

Trenberth, K. E., 1998: Atmospheric moisture residence times and cycling: implications for rainfall rates and climate change. *Climatic Change*, **39**, 667-694.

Trenberth, K., E., 1994: Decadal atmosphere-ocean variations in the Pacific. *Climate Dynamics*, **9**, 303-319.

Tsonis, A. A., 1996: Widespread increases in low-frequency variability of precipitation over the past century. *Nature*, **382**, 700-702.

Vose, R. S., R. L. Schmoyer, P. M. Steurer, T. C. Peterson, R. Heim, T. R. Karl, and J. Eischeid, 1992: The Global Historical Climatology Network: long-term monthly temperature, precipitation, sea level pressure, and station pressure data. ORNL/CDIAC-53, NDP-041. Carbon Dioxide Information Analysis Center, Oak Ridge National Laboratory, Oak Ridge, Tennessee.

Wentz, F. J, and M. Schabel, 2000: Precise climate monitoring using complementary satellite data sets. *Nature*, **403**, 414-416.

Wentz, Frank J. and Roy W. Spencer, 1998: SSM/I Rain Retrievals within a Unified All-Weather Ocean Algorithm, *Journal of the Atmospheric Sciences*, **55**, 1613-1627.

Wielicki, B. A., T. Wong, R. P. Allan, A. Slingo, J. T. Kiehl, B. J. Soden, C. T. Gordon, A. J. Miller, S.-K. Yang, D. A. Randall, F. Robertson, J. Susskind, and H. Jacobowitz, 2002: Evidence for large decadal variability in the tropical mean radiative energy budget.

Science, **295**, 841-844.

Williams, E. and N. Renno, 1993: An analysis of the conditional instability of the tropical atmosphere. *Mon. Wea. Rev.*, **121**, 21-36.

Wilheit, T.T., A.T.C. Chang, L.S. Chiu, 1991. Retrieval of monthly rainfall indices from microwave radiometric measurements using probability distribution functions. *J. Atmos. Oceanic Tech.*, **8**, 118-136.

Xu, K.-M., and K. A. Emanuel, 1989: Is the tropical atmosphere conditionally unstable? *Mon. Wea. Rev.*, **117**, 1471-1479.

Ye, B., A. D. Del Genio, K. K.-W. Lo, 1998: CAPE variation in the current climate and in a climate change. *J. Climate*, **11**, 1997-2015.

List of Figures

Figure 1: CAPE trends computed from sounding data from 1973-1999 for a) 00Z launch times and b) 12Z launch times. Upward- (downward-) pointing triangles denote positive (negative) trends and filled (open) triangles denote trends that are (are not) statistically significant at the 95% confidence level. Trends are indicated above triangles and are expressed as a percentage of their 1973-1999 mean values. Station names are noted below triangles.

Figure 2: Percent of CAPE trend at a) 00Z and b) 12Z explained by precipitable water and surface-to-700 mb lapse rate trends. Positive CAPE trends are indicated by warm colors (magnitude increases from yellow to red colors); negative trends by cool colors (magnitude increases from aquamarine to dark blue colors). Filled (open) symbols denote stations where CAPE trends are (are not) statistically significant. Circles denote stations where both PW and lapse rates are statistically significant; diamonds indicate stations where either PW or lapse trends do not pass the 95% confidence level significance threshold. See text for additional discussion.

Figure 3: a) Relationship of 1973-1999 CAPE trends vs. same period trends in PW and lapse rate, expressed as % change of period mean per decade. Open (filled) symbols denoted CAPE trends that are not (are) statistically significant at the 95% confidence level. Positive (negative) CAPE trends or values are indicated by warm (cool) colors. b) annual cycles of CAPE vs. PW and lapse rate at each sounding station. Open (filled) symbols denote months with rainfall < (>) 100 mm/month. Cool (warm) colors denote low (high) absolute CAPE values. Both 00Z and 12Z data are plotted. c) normalized monthly PW and lapse rate anomalies for months with rainfall > 3 mm/day. Blue (red) symbols denote negative (positive) CAPE anomalies. Linear regressions for each population are shown with solid lines. d) as in 2c), but for months with rainfall < 2 mm/day.

Figure 4: 1973-1999 CAPE trends (triangles) and gridded precipitation trends (circles) based on GHCN surface raingauge data. Filled (open) symbols denote trends that are (are not) statistically significant, while red (blue) symbols denote positive (negative) trends.

Figure 5: Scatter plot of 1973-1999 CAPE trends and nearest grid point GHCN precipitation trends shown in Fig. 4. Dashed lines mark 1:1 and 1:-1 lines. Stations are coded as follows: P-Pacific, C-Caribbean, A-Asia and Australia, S-South America, F-Africa, O-other locations.

Figure 6: Distribution of temporal correlations of several variables at individual sounding locations. Histogram bin widths are 0.2 in all panels. a) sounding-derived PW vs. SSM/I PW, b) sounding-derived CAPE and sounding-derived lapse rate, c) sounding-derived CAPE vs. sounding-derived PW, d) sounding-derived CAPE vs. SSM/I PW, e) SSM/I PW vs. GPCP precipitation, and f) sounding-derived CAPE vs. GPCP rainfall.

Figure 7: Monthly anomaly time series of mean tropical quantities: a) mean ocean-only SSMI PW anomalies, (mm), b) mean sounding-derived precipitable water anomalies (mm), c) land-only GPCP precipitation anomalies (mm/day), d) mean sounding-derived CAPE anomalies (J kg^{-1}), e) ocean-only GPCP precipitation anomalies (mm/day) from 25^{o}N to 25^{o}S.

Table 1: Sounding stations and period of analysis (*=significant trend)

Station name	Begin date M-D-YYYY	End date M-D-YYYY	00Z trend (%/decade)	12Z trend (%/decade)
Abidjan	1-1-1976	12-31-1999		20*
Antofagasta	1-1-1973	12-31-1999		-31*
Ascension	1-1-1973	12-31-1999		29*
Bangkok	1-1-1973	12-31-1999	7*	
Brasilia	1-1-1973	12-31-1999		-2
Broome	1-1-1975	12-31-1999	-7	
Costa Rica	1-1-1974	12-31-1999		-9
Dakar	1-1-1973	12-31-1999		-10
Darwin	1-1-1975	12-31-1999	0	
Funafuti	1-1-1975	12-31-1992	-39*	
Giles	1-1-1973	12-31-1999	10	
Grantley Adams	1-1-1973	12-31-1999	33*	29*
Guam	1-1-1973	12-31-1995	16*	17*
Hilo	1-1-1973	12-31-1999	21*	14*
Key West	1-1-1973	12-31-1999	8*	4*
Kings Park	1-1-1973	12-31-1999	-8*	-8*
Kingston	1-1-1973	12-31-1999	26*	32*
Koror	1-1-1973	12-31-1995	3	
Majuro	1-1-1973	12-31-1999	11*	
Minamitorishima	1-1-1973	12-31-1999	-24*	-6*
Niamey	1-1-1975	12-31-1999		-34*
Niarobi	1-1-1975	12-31-1999		-19*
Noumea	1-1-1976	12-31-1999	4	
Pago Pago	1-1-1973	12-31-1995	12*	10*
San Juan	1-1-1980	12-31-1999	8*	12*
Sao Paulo	1-1-1973	12-31-1999		-12
Seychelles	1-1-1980	12-31-1999		-15*
Tahiti	1-1-1973	12-31-1999	3	
Tarawa	1-1-1975	12-31-1996	4	
Townsville	1-1-1975	12-31-1999	-15	
Truk	1-1-1973	12-31-1999	2	

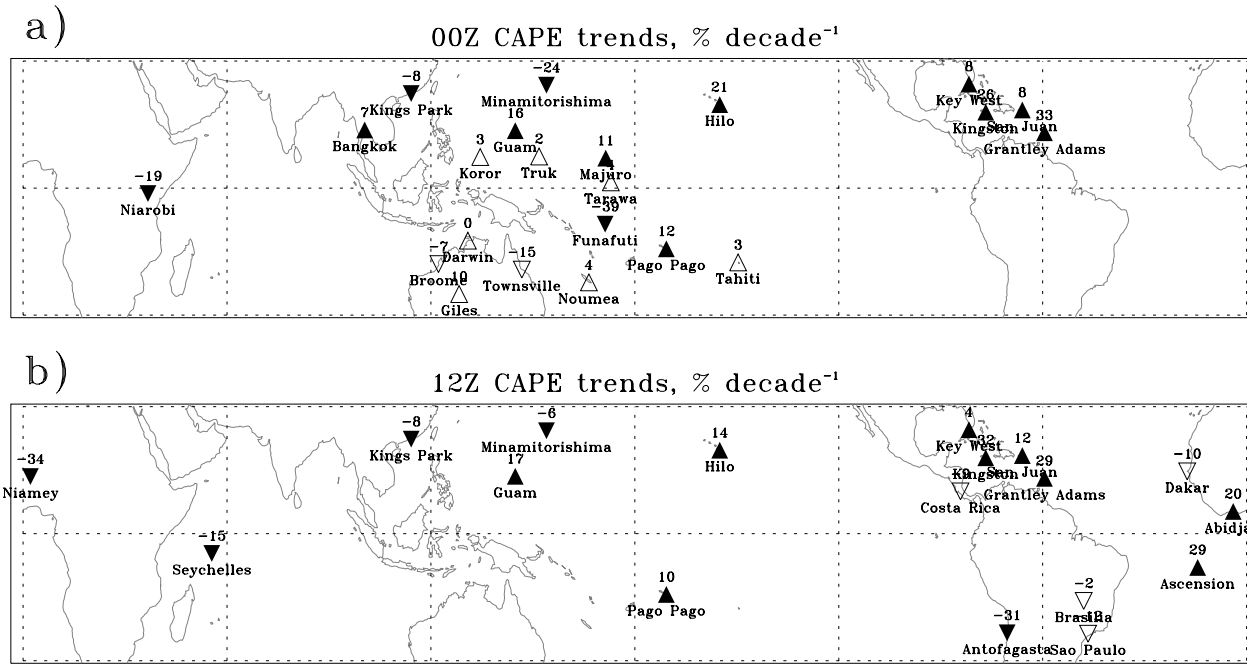

Figure 1: CAPE trends computed from sounding data from 1973-1999 for a) 00Z launch times and b) 12Z launch times. Upward- (downward-) pointing triangles denote positive (negative) trends and filled (open) triangles denote trends that are (are not) statistically significant at the 95% confidence level. Trends are indicated above triangles and are expressed as a percentage of their 1973-1999 mean values. Station names are noted below triangles.

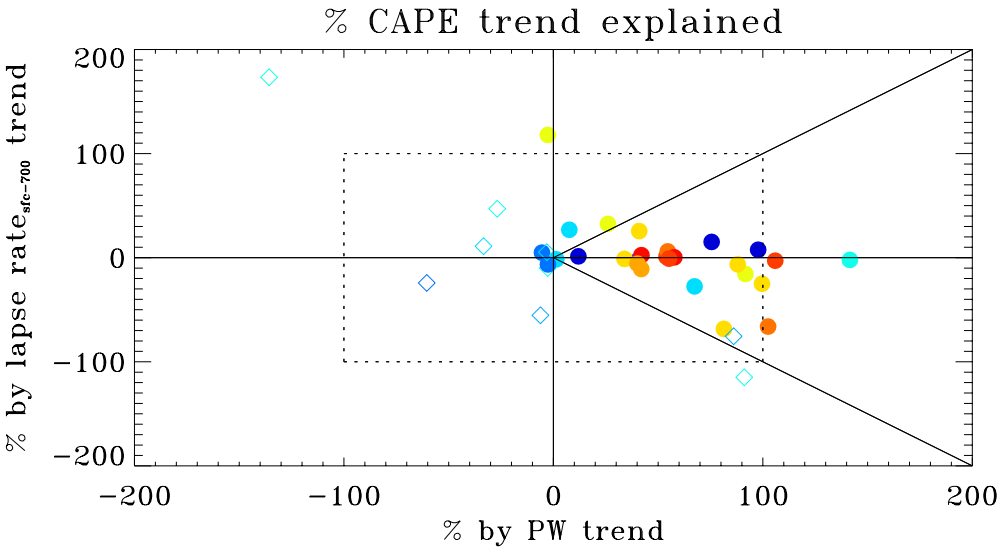

Figure 2: **Percent of CAPE trend explained by precipitable water and surface-to-700 mb lapse rate trends. Positive CAPE trends are indicated by warm colors (magnitude increases from yellow to red colors); negative trends by cool colors (magnitude increases from aquamarine to dark blue colors). Filled (open) symbols denote stations where CAPE trends are (are not) statistically significant. Circles denote stations where both PW and lapse rates are statistically significant; diamonds indicate stations where either PW or lapse trends do not pass the 95% confidence level significance threshold. See text for additional discussion.**

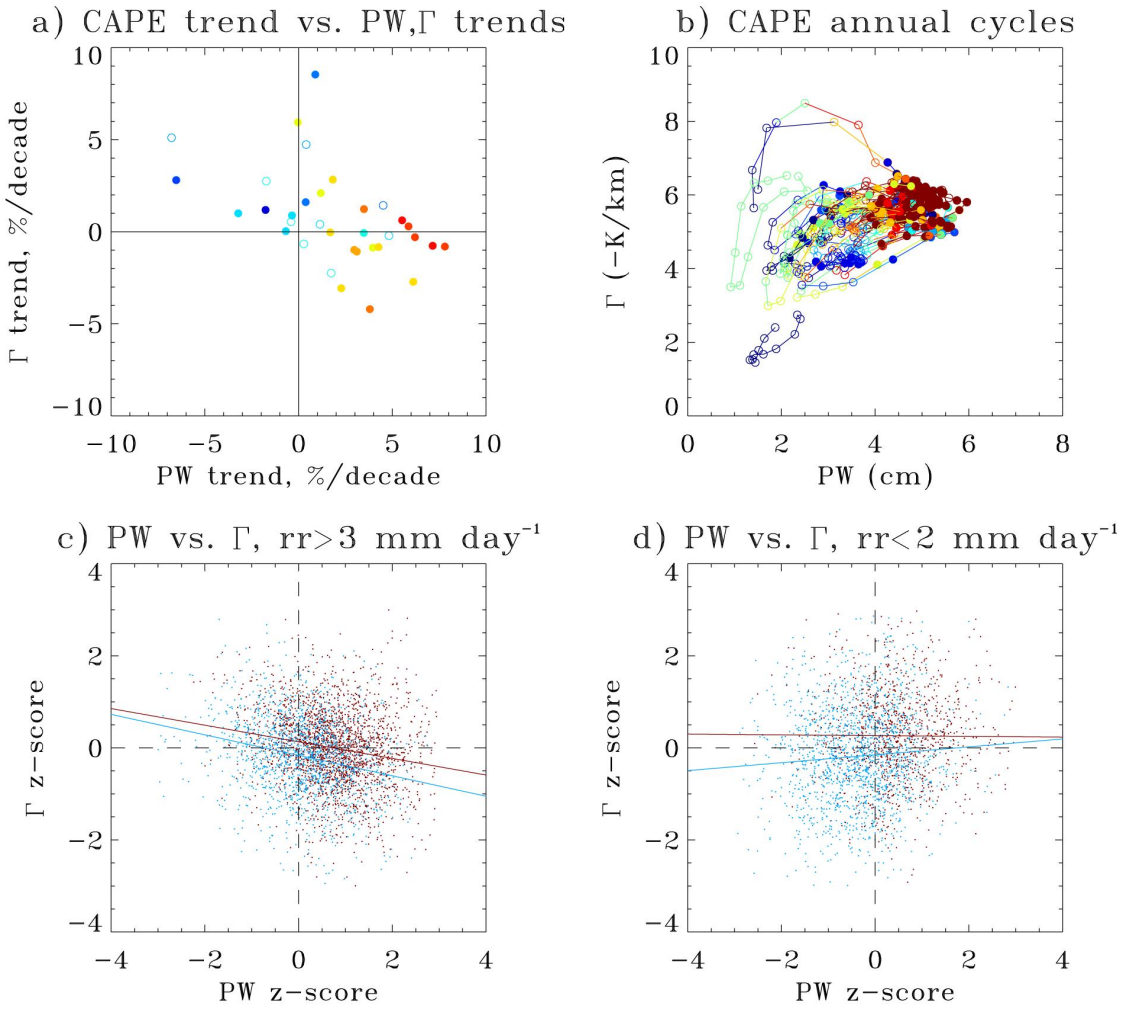

Figure 3: **a) Relationship of 1973-1999 CAPE trends vs. same period trends in PW and lapse rate, expressed as % change of period mean per decade. Open (filled) symbols denoted CAPE trends that are not (are) statistically significant at the 95% confidence level. Positive (negative) CAPE trends or values are indicated by warm (cool) colors. b) annual cycles of CAPE vs. PW and lapse rate for each sounding station. Open (filled) symbols denote months with rainfall < (>) 100 mm/month. Cool (warm) colors denote low (high) absolute CAPE values. Both 00Z and 12Z data are plotted. c) normalized monthly PW and lapse rate anomalies for months with rainfall > 3 mm/day. Blue (red) symbols denote negative (positive) CAPE anomalies. Linear regressions for each population are shown with solid lines. d)**

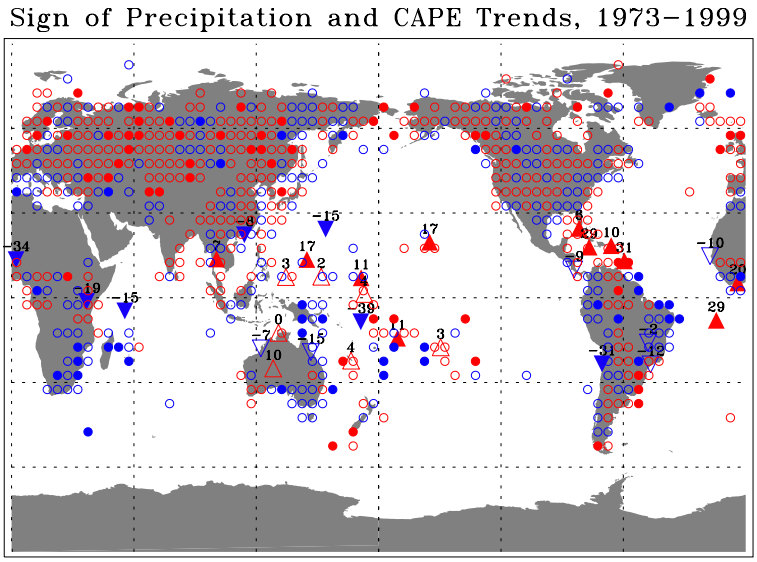

Figure 4: **1973-1999 CAPE trends (triangles) and gridded precipitation trends (circles) based on GHCN surface raingauge data. Filled (open) symbols denote trends that are (are not) statistically significant, while red (blue) symbols denote positive (negative) trends.**

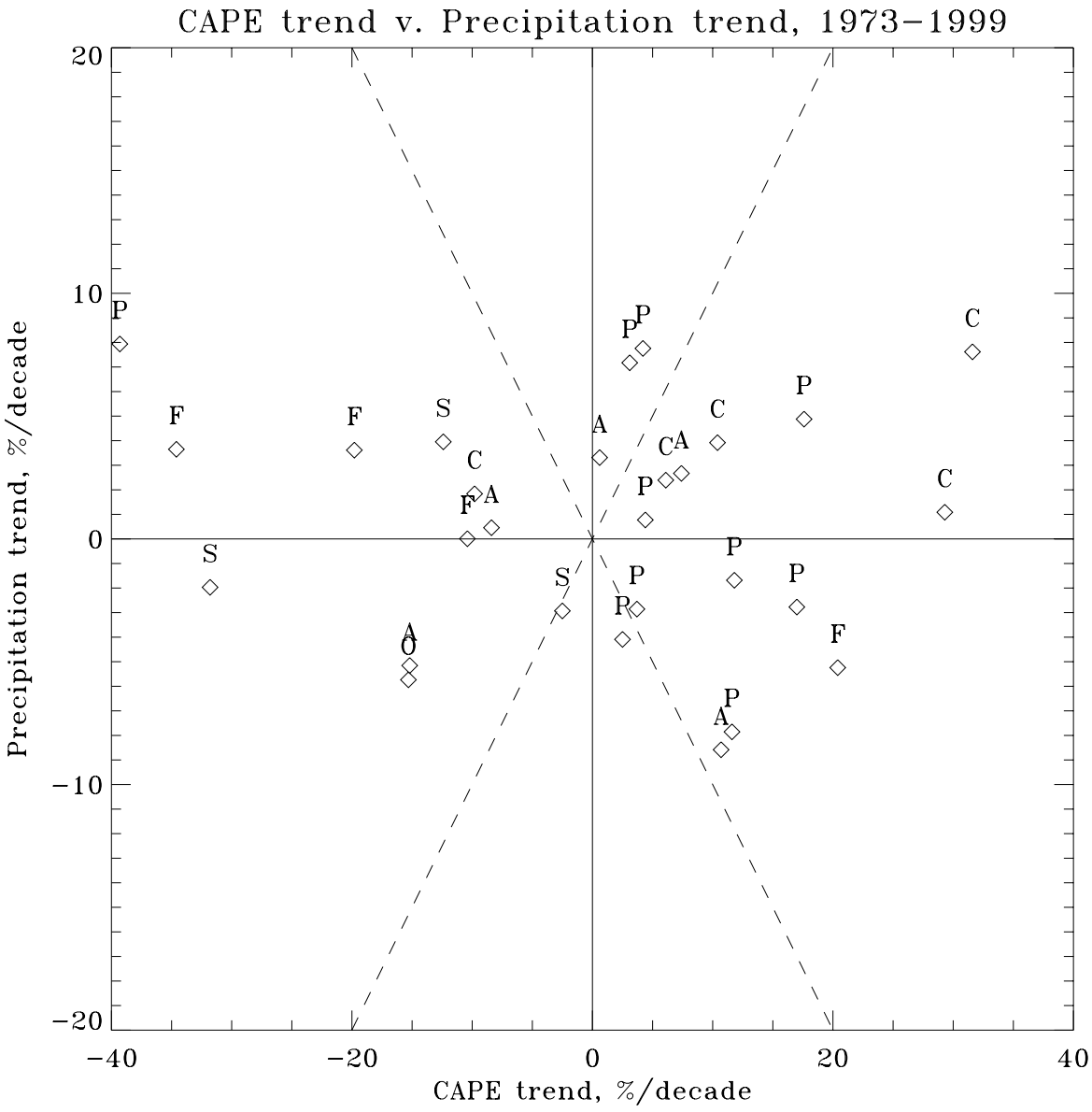

Figure 5: Scatter plot of 1973-1999 CAPE trends and nearest grid point GHCN precipitation trends shown in Fig. 4. Dashed lines mark 1:1 and 1:-1 lines. Stations are coded as follows: P-Pacific, C-Caribbean, A-Asia and Australia, S-South America, F-Africa, O-other locations.

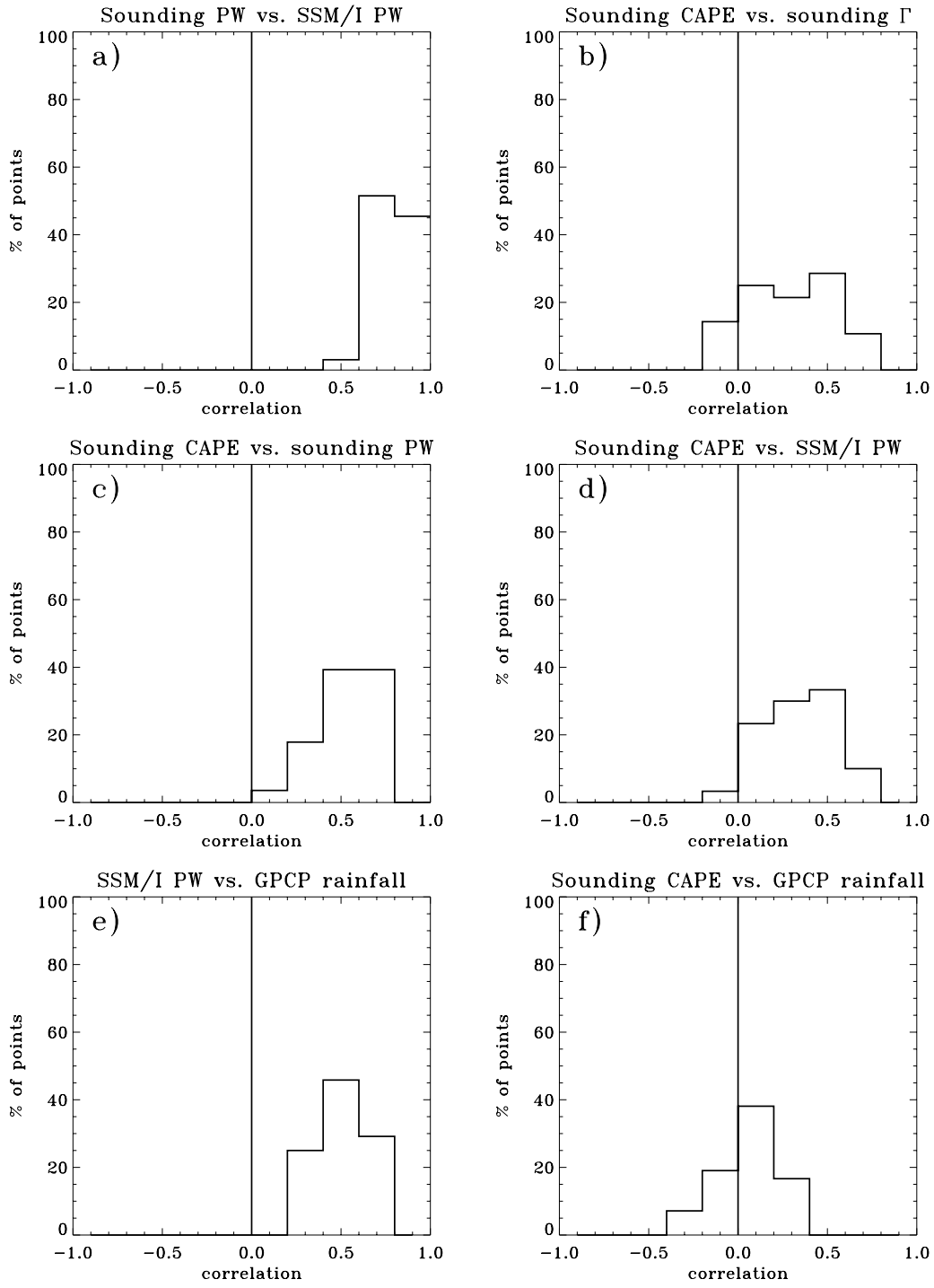

Figure 6: **Distribution of temporal correlations of several variables at individual sounding locations. Histogram bin widths are 0.2 in all panels. a) sounding-derived PW vs. SSM/I PW, b) sounding-derived CAPE and sounding-derived lapse rate, c) sounding-derived CAPE vs. sounding-derived PW, d) sounding-derived CAPE vs. SSM/I PW, e) SSM/I PW vs. GPCP precipitation, and f) sounding-derived CAPE vs. GPCP rainfall.**

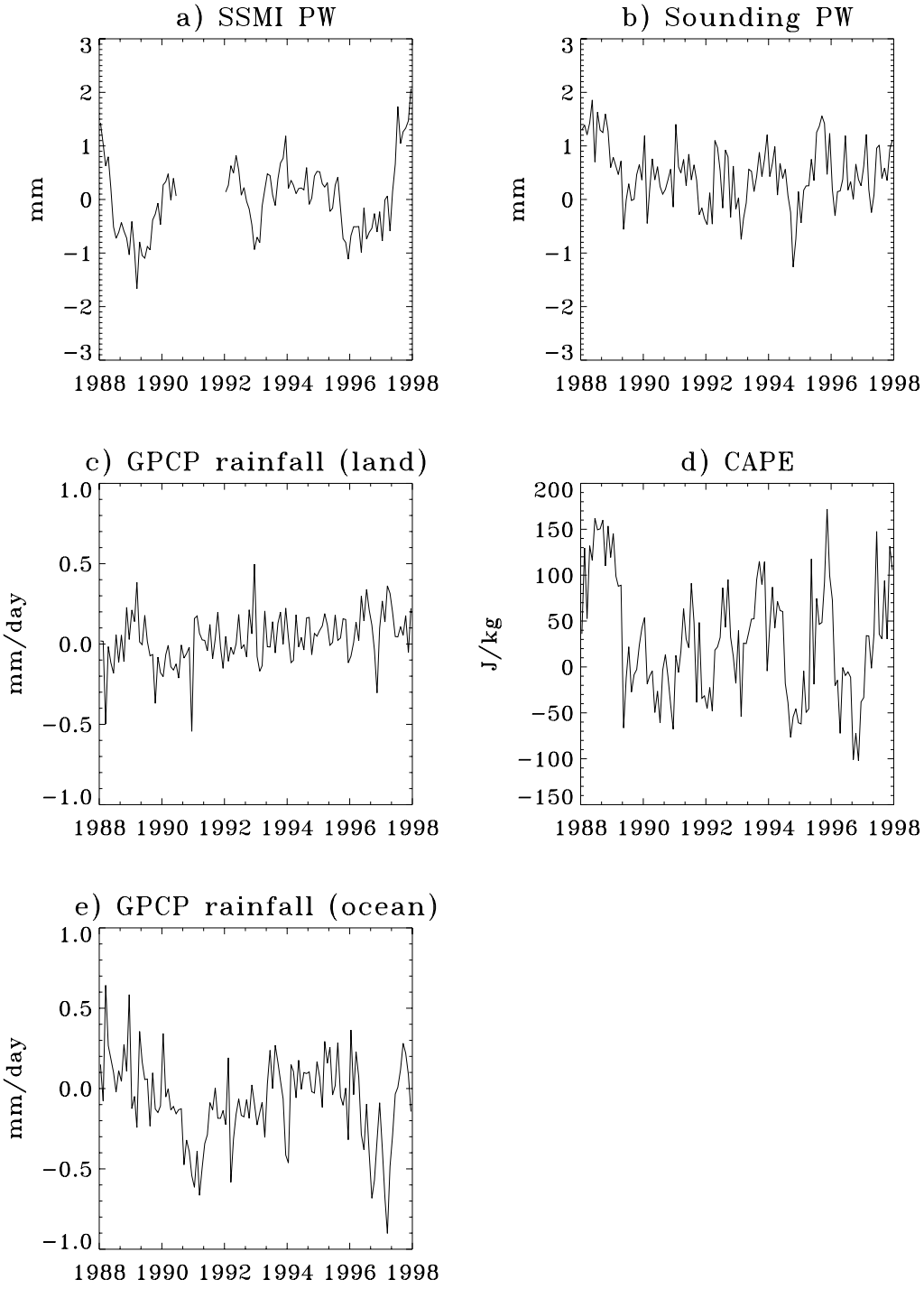

Figure 7: **Monthly anomaly time series of mean tropical quantities: a) mean ocean-only SSMI PW anomalies, (mm), b) mean sounding-derived precipitable water anomalies (mm), c) land-only GPCP precipitation anomalies (mm/day), d) mean sounding-derived CAPE anomalies (J kg^{-1}), e) ocean-only GPCP precipitation anomalies (mm/day) from 25^{o}N to 25^{o}S.**